

# PROCEEDINGS OF SPIE

[SPIDigitalLibrary.org/conference-proceedings-of-spie](https://SPIDigitalLibrary.org/conference-proceedings-of-spie)

## Automated stent defect detection and classification with a high numerical aperture optical system

Bermudez, Carlos, Laguarda, Ferran, Cadevall, Cristina, Matilla, Aitor, Ibañez, Sergi, et al.

Carlos Bermudez, Ferran Laguarda, Cristina Cadevall, Aitor Matilla, Sergi Ibañez, Roger Artigas, "Automated stent defect detection and classification with a high numerical aperture optical system," Proc. SPIE 10334, Automated Visual Inspection and Machine Vision II, 103340C (26 June 2017); doi: 10.1117/12.2275614

**SPIE.**

Event: SPIE Optical Metrology, 2017, Munich, Germany

# Automated stent defect detection and classification with a high numerical aperture optical system

Carlos Bermudez<sup>\*ab</sup>, Ferran Laguarda<sup>a</sup>, Cristina Cadevall<sup>ab</sup>, Aitor Matilla<sup>b</sup>, Sergi Ibañez<sup>c</sup>, Roger Artigas<sup>ab</sup>

<sup>a</sup>Technical University of Catalonia (UPC), Center for Sensors, Instruments and Systems Development (CD6), Rambla Sant Nebridi 10, Terrassa, Spain, E-08222; <sup>b</sup>Sensofar-Tech, S.L., Ctra. BV1274 km 1, Terrassa, Spain, E-08225; <sup>c</sup>Sensofar-Medical, S.L., Ctra. BV1274 km 1, Terrassa, Spain, E-08225

## ABSTRACT

Stent quality control is a highly critical process. Cardiovascular stents have to be inspected 100% so as no defective stent is implanted in a human body. However, this visual control is currently performed manually and every stent could need tenths of minutes to be inspected. In this paper, a novel optical inspection system is presented. By the combination of a high numerical aperture (NA) optical system, a rotational stage and a line-scan camera, unrolled sections of the outer and inner surfaces of the stent are obtained and image-processed at high speed. Defects appearing in those surfaces and also in the edges are extremely contrasted due to the shadowing effect of the high NA illumination and acquisition approach. Therefore by means of morphological operations and a sensitivity parameter, defects are detected. Based on a trained defect library, a binary classifier sorts each kind of defect through a set of scoring vectors, providing the quality operator with all the required information to finally take a decision. We expect this new approach to make defect detection completely objective and to dramatically reduce the time and cost of stent quality control stage.

**Keywords:** stent inspection, machine vision, visual control, image processing, surface defects, defect classification

## 1. INTRODUCTION

In recent years stent manufacturing is growing exponentially and several market research analyses foresee its increase in upcoming years. Stents are implantable medical devices made from metallic or polymeric tubes. They are designed to remove blood restrictions or to temporarily allow access for surgery applying mechanical forces when it is expanded through a balloon catheter. Stent geometry consists of a mesh structure of struts which has been specially designed to perform certain mechanical deformations to the vessels without causing any damage to the patient or the inflation balloon. Any defect in the geometry or in the surface can reduce the effectiveness or even cause a life-threatening situation. Therefore stent inspection, which is being performed nowadays as a manual visual inspection, is of extreme importance to assure their quality.

Existing stent inspection systems provide both critical dimension (CD) analysis and defect detection. Nevertheless, they usually produce low-resolution images and sidewalls height analysis is performed by contact means. This paper describes an optical inspection system that combines a high numerical aperture imaging scheme with a triple lighting illumination approach which performs CD analysis, defect detection and classification from the outer, inner and sidewalls surfaces<sup>1,2</sup>. High quality is achieved thanks to well-focused, high-contrast images. Stent is placed on a high-precision rotational stage to obtain unrolled images of its surfaces. For those stents with irregular shapes we show the development of a mandrel system which allows imaging the inner surface with high contrast.

The remainder of this paper is organized as follows: In next section, stent manufacturing process and defect detection state-of-the-art will be introduced. The design of the inspection system is proposed in Section 3. Automated defect detection approach is described in Section 4 whereas Section 5 introduces defect classification algorithm. Finally, conclusions appear in Section 6.

\*bermudez@sensofar.com;

phone +34 93 700 14 92;

www.sensofar.com

Automated Visual Inspection and Machine Vision II, edited by Jürgen Beyerer,  
Fernando Puente León, Proc. of SPIE Vol. 10334, 103340C · © 2017 SPIE  
CCC code: 0277-786X/17/\$18 · doi: 10.1117/12.2275614

Proc. of SPIE Vol. 10334 103340C-1

## 2. STENT MANUFACTURING

Vascular stents can be classified into two categories: coronary and peripheral stents. Coronary stents are those to be implanted inside the heart whereas peripheral stents could be released in any other artery or vessel of the human body. Initially, stents were manufactured with raw metals, such as stainless steel and chromium-cobalt, but they were quickly improved with coatings to avoid restenosis<sup>3</sup>, converted in what is nowadays called a drug-eluting stent (DES). Other materials are being used more recently, such as nitinol, which has shape memory, or polymers, which can be bio-absorbed<sup>4</sup>.

The manufacturing process of a stent consists of several steps: first, the raw tubes are laser-cut. Then the remainders of the laser cut are removed through a pickling stage and finally a dimensional verification is performed. After this step, stents receive a surface treatment and a coating may be applied. The latest step is to make a final quality inspection to assure the stent has neither faulty critical dimensions nor defects before its implantation process.

### 2.1 Stent visual inspection

Defects may occur along every manufacturing step and handling. Stent inspection is therefore an extremely important process, its surfaces are required to be inspected carefully in order to detect deviations in strut critical dimensions, to detect defects and to check the consistent and even distribution of coatings. This process is nowadays highly labor-intensive, time-consuming and expensive, carried out by skilled operators assisted by optical magnification tools, who will take the final decision. A stent is accepted or rejected based in their own judgment and experience, eventually yielding faulty stents due to human errors.

Defects in stents are quality mismatches that could endanger stent performance. They could appear either on the surface or inside the stent material, which can only be detected through X-ray and MRI instruments. Defects may arise also during laser cutting and etching<sup>5</sup>, although some of them can be embedded during stent tube manufacturing and then appear during the stent production process<sup>6</sup>.

An automatic vision-based inspection system offers repeatability and objectivity. Nowadays, there are only a few automated stent inspection systems. Ibraheem<sup>7</sup> developed a line-scan approach to obtain relatively high resolution images (31 $\mu$ m lateral resolution) combined with a critical dimension analysis but with no defect detection capability. Freifeld<sup>8</sup>, on the other side, accumulates a large amount of patents for a system which also uses a line-scan camera to analyze critical dimensions on struts as well as edge defect detection algorithms.

### 2.2 Defect detection and classification

However, there is the lack of a high-resolution stent inspection system to detect defects in all surfaces, including outer, inner and sidewalls. A similar application of defect inspection is found in the ceramic tile<sup>9,10</sup> or printed circuit board (PCB) industries. Ceramic tiles are produced in a fully-automated manufacturing chain, being good quality and high production rate compulsory. However, inspection is still manual and very similar nomenclature as in the stent industry is used<sup>9</sup>.

The most common approach that allows identifying defects and at the same time remove noise and background is with the use of morphological image processing. Morphology is widely used not only in ceramics<sup>11</sup>, but also in other industry segments where surface defects may appear<sup>12-14</sup>.

Once candidates are detected, it is of extreme importance to classify them in order to further investigate their causes and to improve the production processes.

As opposed to other industry fields where automated machine inspection solutions are developed, stent defect classification has still to be developed.

Some industrial defect classifiers are the ones based on pattern recognition such in the PCB industry, where the segmented image is compared to a model and defects are discriminated according to the place where they appear<sup>15</sup>, but cannot be applied in samples whose defects may arise anywhere in the stent surface or edge.

For that reason, we will propose a supervised classification system based on a previous knowledge of the classes of defects that could appear. This learning will be provided to the system by an expert inspector in a training process<sup>16,17</sup>.

### 3. OPTICAL INSPECTION SYSTEM

Defects may be described as local variations of the surface slope which are deviations from the expected shape. The best way to detect those local irregularities through optical means is by the use of a high numerical aperture optical system in order to increase lateral resolution but sufficiently low in order to maximize local contrast, therefore to improve the detectivity. Fig. 1 shows a strut defect imaged with three different NAs. Although low NA (0.15) does not provide highest lateral resolution, the defect is clearly seen (a), while with higher NA (0.45) dramatically decreases local contrast in that region (c). We can assume that 5X 0.15NA lens provide high detectivity and a sufficient lateral resolution, covering the largest field of view to increase inspection throughput.

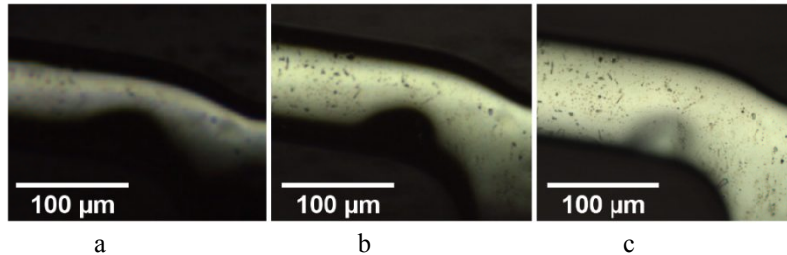


Figure 1. 30µm mouse bite edge defect. Images taken with different microscope objectives: (a) 5X 0.15NA, (b) 10X 0.2NA and (c) 20X 0.45NA.

Defects may appear on the stent surface as very small features. They could be very difficult to detect with traditional telecentric camera systems or microscope arrangements. An optimal-NA imaging system combined with an epi-illumination scheme would receive more light from flat areas on the surface rather than those local slope variations (Fig. 2b), pointing out defects in a straightforward way which are not visible using diffuse illumination (Fig. 2a).

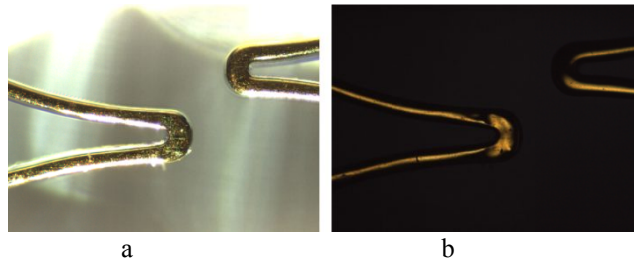


Figure 2. Stent strut images obtained with a 5X 0.15NA lens (a) diffuse illumination, (b) epi-illumination.

Moreover, since a stent is cut from a cylindrical tube, assessing the quality of the cutting process is of interest. To do so, an Epi-illumination system has to be combined with another illumination mean such as a green-color diffuse back-illumination (Fig. 3) which would provide geometry information, such as strut width, or even point out defects located in the strut edge (Fig. 4). An additional diffuse light source will be used for further investigation regarding to sidewalls imaging.

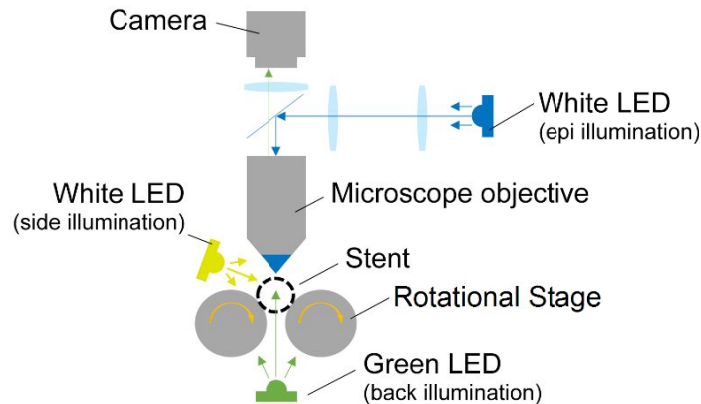


Figure 3. Triple lighting system arrangement.

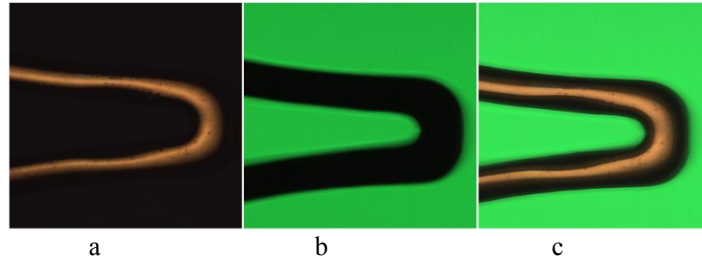


Figure 4. Electropolishing defect. (a) Epi-illumination only, (b) Back-illumination only, (c) Epi- and Back- illumination.

Although 2D imaging provides lateral information of the defect, it is sometimes needed to perform a 3D measurement of the defects, for instance to solve the ambiguity of a defect being a hole or a bump, information which is not provided by the 2D image. In the same microscope arrangement, an interferometric objective can be used together with Coherence Scanning Interferometry (CSI) technique to recover said 3D shape (Fig. 5)<sup>18</sup>. This 3D capability is also extremely useful for measuring the coatings thickness in drug eluting stents<sup>19</sup>.

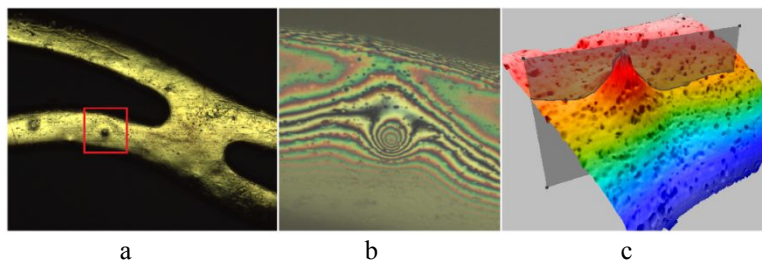


Figure 5. (a) Ambiguous  $\text{\O}25\mu\text{m}$  defect (hole-bump), (b) Interferometric fringes, (c) 3D shape, tip is only  $2\mu\text{m}$  in height.

## 4. AUTOMATED DEFECT DETECTION

### 4.1 Mask Generation

In order to assess the quality of stents, the whole sample has to be inspected. Therefore, the acquisition system has to be able to inspect its cylindrical shape all along its length with high resolution. In a high numerical aperture system, bright field image only provides useful information from the area which is normal to the optical axis, that is the stent apex, the rest of the image is dark and out of focus. To obtain information along the whole stent perimeter, a line-scan approach has been implemented which leads to a stent “section” (Fig. 6). The whole stent image acquisition process therefore is to obtain several unrolled section images within an axial movement along the stent diameter. The same process is applied for imaging the inner diameter.

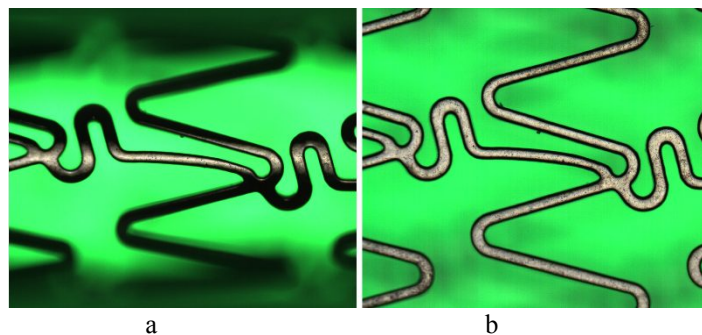


Figure 6. Stent strut images taken with a 5X 0.15NA lens, (a) bright field screenshot, (b) part of a line-scan acquired section.

Once we obtain high-resolution and well-focused images, stent detection is a matter of image processing. In a stent, defects may arise both in its surfaces (inner or outer) such as holes, bumps, scratches, etc. and in the edges, for instance mouse bites, uneven electropolishing, fractures, etc.

First, in order to select the foreground from the background, a binary mask has to be constructed. Since the background is green, the subtraction of the red channel from the green one leads to an image that can be directly histogram-thresholded to obtain its mask (Fig. 7a, b and c). Moreover, to obtain the surface mask it is only needed to threshold the grayscale image filtered by the former outer mask (Fig. 7d, e and f).

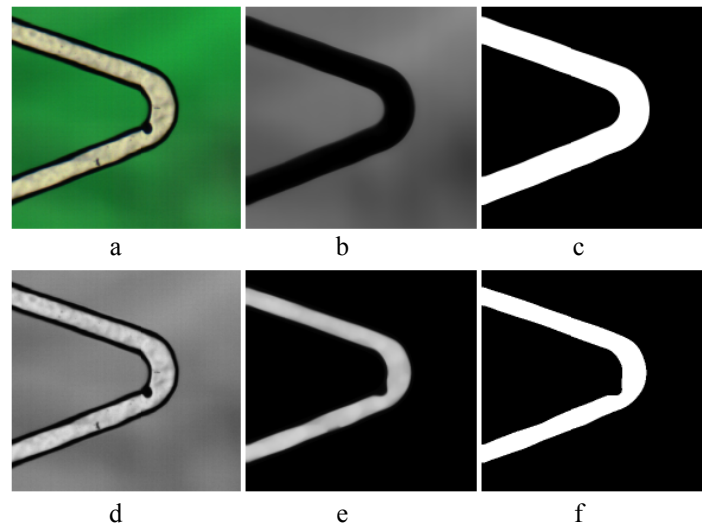


Figure 7. Strut with a crack defect, (a) bright field, (b) green minus red channel, (c) outer mask, (d) grayscale image, (e) masked grayscale image, (f) surface mask.

In addition to the surface mask, it is also of interest the capability to detect defects located in the strut edges. Edge mask can be generated from outer and inverted surface mask, as can be seen in Fig. 8:

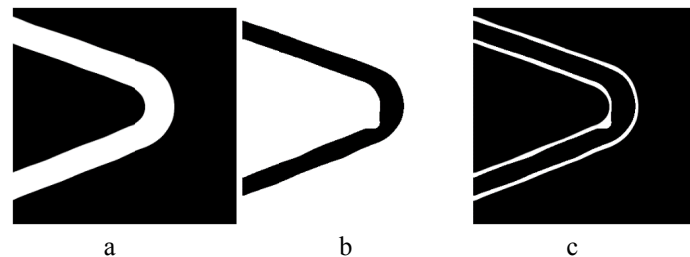


Figure 8. Edge mask generation, (a) outer mask, (b) inverted surface mask, (c) edge mask.

Outer mask performance is based on subtracting the red channel from the green channel, so it is sensitive to the stent surface color. Most stents are made of metal alloys, appearing frequently white or yellowish. However, polymer stent manufacturing is increasing dramatically in recent years, and metal stents can also be coated with different materials, mostly drugs. In those cases, stent surface exhibits rainbow colors due to coating interferences, producing incorrect binary masks (Fig. 9a and b).

Thereby, it is needed a color processing before the mask generation. In our case we have performed a color space transformation from RGB to HSV. Within the Hue channel, a small green range (between 70° and 145°) have been mapped to pure green (120°) while all the other colors have been mapped to pure red (0°). After a back conversion to RGB, resulting image can be processed as mentioned before (Fig. 9c and d).

This color conversion approach will work as long as there is no green color in the stent surface. In such case, two different options can be performed to fill hollow areas within the surface (Fig. 9b): change the background light source color or make the mask generation algorithm insensible to foreground color change, which is out of the scope of this study.

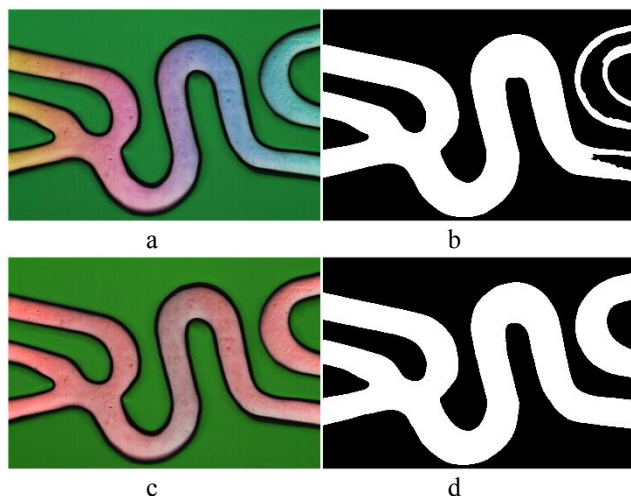


Figure 9. Drug-eluting stent, with a scratch on top, (a) bright field image, (b) incorrect outer mask, (c) color transformed image, (d) outer mask.

## 4.2 Candidate Generation

Once the image to be analyzed has been preprocessed and its masks obtained, a defect detection algorithm, both in strut surface and edges, can be applied. As exposed in Sec. 2, defects may appear as local grayscale variations due to the surface slope imaged with the adequate NA. For that reason, morphological operations within the set of images and masks will depict all the local deviations.

### 4.2.1 Surface defects

For a surface defect analysis, we start from the grayscale original image masked with the surface mask (Fig. 10b), where a morphological closing is applied (Fig. 10c), the difference image (Fig. 10d) shows all the surface irregularities.

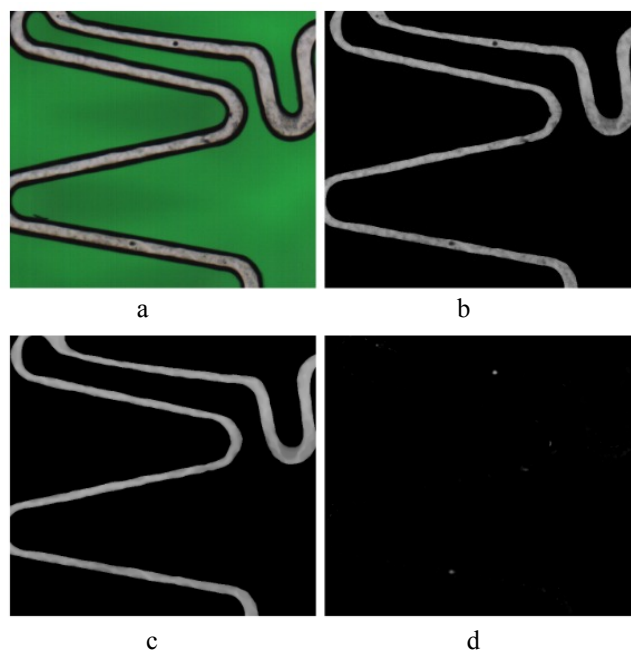


Figure 10. Strut with holes, (a) bright field image, (b) grayscale image filtered with surface mask, (c) applied a morphological closing to (b), (d) difference image (c-b).

Surface irregularities cannot be directly assigned as defect candidates since there will be a lot of false positive. Therefore a further filtering is needed, not only by a grayscale threshold (which will depict well-contrasted defects) but also by an

area filtering, highlighting only big defects. Both parameters can be defined as a function of a sensitivity adjustment, so stent manufacturer could determine which ones are defects or false positives.

A final blob detection tool parametrized with such characteristics will point out the final defect candidates (Fig. 11).

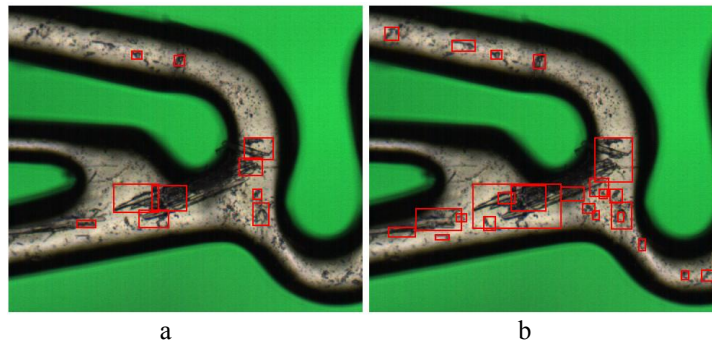


Figure 11. Neural stent with a pitting defect, (a) low sensitivity, (b) high sensitivity.

#### 4.2.2 Edge defects

As in surface defect detection, morphological operations have been applied in the edge mask to detect edge irregularities. Defects appearing in the strut edges can be located in two regions: in the “inner edge”, or in the “outer edge”. The former ones are those which lay in the limit between the strut surface and dark (edge) areas like a crack (Fig. 7), so they can be detected through the surface detection method. The latter ones appear within the region between the edge and the background.

An outer edge defect is the one appearing in Fig. 12. In this case it is a cutting or etching misprocessing, which formed a defect type known as a spine (a).

In order to detect irregularities in the strut limit or outer edge, a median filter has been applied 10 times to the edge mask (b). Filtered mask appears in (c) after 10 iterations. In every iteration, the difference between the mask before and after filtering (d) is accumulated into an additive buffer, which in the end has all the sharp deformation signal (e).

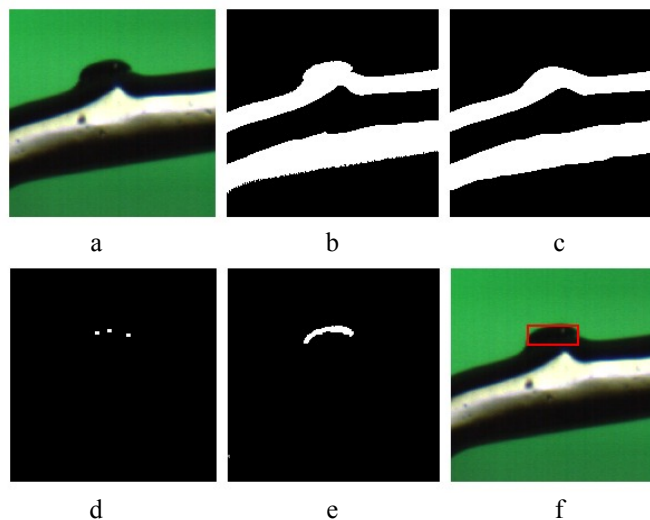


Figure 12. Strut with a spine defect, (a) bright field, (b) edge mask, (c) median filter applied to (b) after 10 iterations, (d) difference between (b) and (c) in one single iteration, (e) sum of (d) along all the iterations to form a candidate, (f) defect candidate highlighted.

## 5. DEFECT TRAINING AND CLASSIFICATION

Stent defects may appear in any region of the image, although we will have always a controlled scenario: candidates will be dark features within a stent strut, together with a green background and a bright foreground. This leads to the design of a classifier with geometrical characteristics, such as aspect ratio, angle, diameter, color, etc.

There is no standard defect nomenclature as every stent manufacturer call them with a particular subjective name, although the most common ones are usually denominated with typical machine vision defect types such as scratches, holes, mouse bites, fractures, etc.

To classify every defect candidate to each defect type, a multiclass classifier scheme has been implemented. However, since a different detection method has to be applied due to the nature of the defect, each method will have its own classifier. Fig. 13 shows how a defect is detected and its features quantified. Afterwards, it receives a score depending on its scoring function and it is finally classified according to the maximum score.

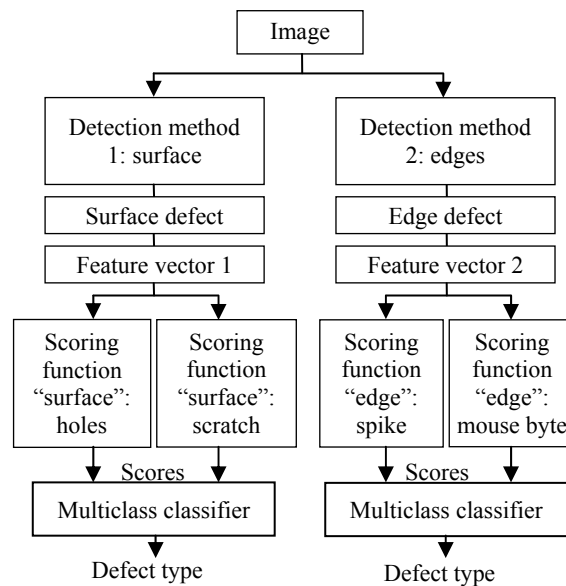


Figure 13. Detection and classification flow.

### 5.1 Training

Scoring functions have to be trained for every defect type (hole, mouse byte, etc.) A supervised learning scheme is needed. The user labels a defect type or class and inputs a set of images of this type as a reference to build up an average Feature vector.

The supervised training algorithm has to be trained with enough representative samples of the defect type, with careful selection that allows a good representation of the defect type. Classifier performance will then depend on such training, where outliers should be avoided in this process in order not to deviate its performance.

We have developed a feature vector for surface detection method described in 4.2.1. Using the defect aspect ratio we can distinguish between a hole and a scratch, and with the angle direction we can determine the orientation of the scratch. We have prepared a set of each defect (hole, horizontal scratch and vertical scratch) to do the training, as can be seen in Fig. 14. First defect in (b) is a dust particle, but its geometry and contrast is very similar to the rest of scratches.

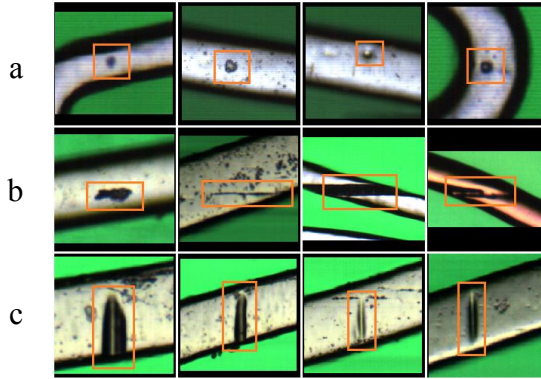


Figure 14. Defect types: (a) Hole, (b) Horizontal scratch, (c) Vertical scratch.

Next step is to define a score function for each dimension in the feature vector, in this case aspect ratio and angle. For those feature types, a discretized Gaussian scoring function has been used, which will center the function to the average value of every feature. Its maximum score limits are defined by  $2\sigma$  and minimums by  $4\sigma$ , being  $\sigma$  the standard deviation of the feature vector. Aspect ratio scoring function ranges from 0 to 1, whereas the angles are confined between  $-45^\circ$  and  $135^\circ$  just for avoiding to split the functions into two parts. Fig. 15 shows the value of each feature for each defect (markers) and the generated scoring function for every defect type (lines).

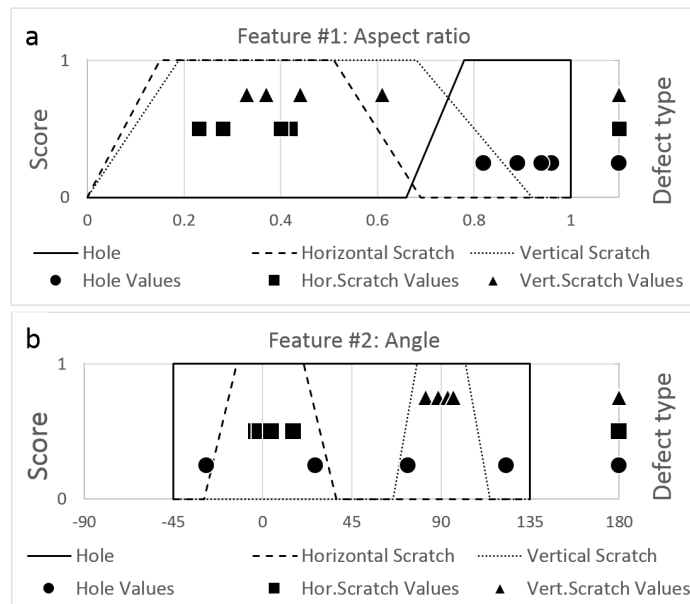


Figure 15. Scoring functions (lines) for three defect classes: Hole, Horizontal scratch and Vertical scratch (markers). (a) Aspect ratio, (b) angle.

## 5.2 Classification

After the training, the classifier is set-up with the rules or scoring functions. Every new detected defect features are scored and the product of such scores is obtained. As can be seen in Table 1, a set of 4 defects have been detected and scored. Whereas numbers #2, #3 and #4 have received a single score from a single scoring function, number #1 receives score from two scoring functions. Multiclass classifier determines the defect type as the one which has the higher score, as represented in Fig. 16. Notice the vertical scratch score of the defect #1, although being over the threshold, hole function score is higher, so this defect is finally classified as a hole. Scores below a certain threshold are directly refused.

Table 1. Scores given to 4 found defects. Shaded cells indicate highest score.

Defect features			Scoring functions		
#	Aspect Ratio	Angle (°)	Hole	Horizontal scratch	Vertical scratch
1	0.83	90	1	0	0.61
2	0.38	91.24	0	0	1
3	0.75	0	0.87	0	0
4	0.15	-9.12	0	0.99	0

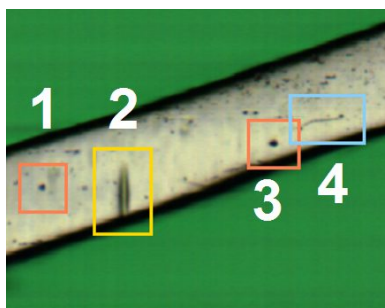


Figure 16. Classified defects (1, 3) Holes, (2) Vertical scratch, (4) Horizontal scratch.

## 6. CONCLUSIONS

In this paper, a new high numerical aperture optical system for stent inspection and defect detection and classification has been presented.

Morphology image processing algorithms have been applied to acquired images so as to detect defects in stent surface and edges. A supervised multiclass classifier has been implemented. After its training, it is able to classify defects into different types.

Future work involves further expansion of feature vectors for all detection methods to be more discriminative in front of any defect type, as well as creating new methods for other defect types.

## REFERENCES

- [1] Bermudez, C., Laguarda, F., Cadevall, C., Matilla, A., Ibañez, I. and Artigas, R., "Stent Optical Inspection System calibration and performance," *OSA Applied Optics*, 56(9) (2017)
- [2] Laguarda, F, Bermudez, C, Artigas, R, Cadevall, C, "Device and method for optically inspecting and analysing stent-like objects," Patent WO2015/096874 A1 (2013)
- [3] Muramatsu, T., et al., "Avances en el tratamiento mediante intervención coronaria percutánea: el stent del futuro," *Revista Española de Cardiología*. 66(6), 483-496 (2013).
- [4] A. Abizaid, J. Ribamar, "New Drug-Eluting Stents. An overview on Biodegradable and Polymer-Free Next-Generation Stent Systems," *Circ Cardiovasc Interv.* 3, 384-393 (2010).
- [5] Katona, B., et al., "Chemical etching of nitinol stents," *Acta of Bioengineering and Biomechanics* 15(4) (2013).
- [6] Quing-fu, C., Wen-Yan, T., "Effect of process inspection on the selection and confirmation of coronary stents tubing," *Journal of Clinical Rehabilitative Tissue Engineering Research* 12(19), 3796-3798 (2008).
- [7] Ibraheem, I., Binder, A., "An automated inspection system for stents," *The International Journal of Advanced Manufacturing Technology* 47, 945-951 (2009).
- [8] Freifeld, D., "Stent inspection system," US Patent 2010/0014747 (2010).

- [9] Elbehiery, A., Hefnawy, A., Elewa, M., "Surface Defects Detection for Ceramic Tiles Using Image Processing and Morphological Techniques," *International Journal of Computer, Electrical, Automation, Control and Information Engineering* 1(5) (2007).
- [10] Sanghadiya, F., Mistry, D., "Surface Defect Detection in a Tile using Digital Image Processing: Analysis and Evaluation," *International Journal of Computer Applications* 116(10) (2015).
- [11] Meena, Y., Mittal, A., "Blobs and Cracks Detection on Plain Ceramic Tile Surface," *International Journal of Advanced Research in Computer Science and Software Engineering* 3(7) (2013).
- [12] Datta, A.K., Chandra J.K., "Detection of Defects in Fabric by Morphological Image Processing," in P. Dobnik (Ed.), *Woven Fabric Engineering* 217-232. Sciyo, Rijeka, Croatia (2010).
- [13] Jiang, C., et al. "Developing a new automatic vision defect inspection system for curved surfaces with highly specular reflection," *International Journal of Innovative Computing, Information and Control* 8(7B) (2012).
- [14] Sarigul. E., Lynn, A., Schmoldt, D.L., "Rule-driven defect detection in CT images of hardwood logs," *Computers and Electronics in Agriculture* 41, 101-119 (2003).
- [15] Chang, P.C., Chen, L.Y., Fan, C.Y., "A case-based evolutionary model for defect classification of printed circuit board images," *Journal of Intelligent Manufacturing* 19, 203-214 (2008).
- [16] Xie, X., "A Review of Recent Advances in Surface Defect Detection using Texture analysis Techniques," *Electronic Letters on Computer Vision and Image Analysis* 7(3) (2008).
- [17] Chmielewski, X., Sklodowski, M., Cudny, W., "Classification of defects on the surface of black ceramics," *AMAS Workshop on Image Analysis in Investigation of Concrete SIAIC'02*, 203-230 (2002).
- [18] de Groot, P., "Coherence Scanning Interferometry," in Leach, R.K., *Optical measurement of surface topography*, 187-206, Springer, Berlin, Germany (2011).
- [19] Bermudez, C., Laguarda, F., Cadevall, C., Matilla, A., Ibañez, I. and Artigas, R., "Optical stent inspection of surface texture and coating thickness," *Proc. SPIE vol. 10110, Photonic Instrumentation Engineering IV*, 1011007 [doi: 10.1117/12.2249614] (2017)